Chapter

2

**Light absorption in a UV-BCR
and
Photolysis of H$_2$O$_2$**

Keep things as simple as possible, but not simpler.
Albert Einstein

2.1 INTRODUCTION

The main distinction between photochemically and thermally activated reactions is the existence of an initiation step, which is a function of the distribution of radiation energy inside the reactor. Therefore, in analyzing the reaction rate of a photochemical reaction, it is necessary to know the exact amount of light energy being absorbed by the reactant. In a bubble type photochemical reactor (such as the one presented in this study) it is not easy to determine the light absorption rates analytically. The problem can be approached in two different ways: (a) by rigorously modeling the process, taking into account the scattering of radiation produced by the heterogeneities of the medium, or (b) by using the existing formulation of a homogeneous media with application of an effective attenuation coefficient. Due to simplicity and recognition in the literature (Alfano *et al*., 1986b, Casano *et al.,* 1995), the effective attenuation approach was selected, using an empirical correlation as proposed by Yokota *et al.* (1981). This work attempts to add some quantitative aspects regarding the prediction of UV light distribution and absorption in liquid and gas – liquid systems in particular, some important parameters that affect the kinetic constant in the UV light driven processes. It will be shown that with properly obtained effective light path length it is possible to predict the average light absorption rates within the photoreactor based on the simple radial model.

2.2 THEORY

In the UV/H_2O_2 process the reaction is induced by the absorption of photons by hydrogen peroxide, which leads to the production of OH radicals, the active species in the photolytic reaction system

$$H_2O_2 + h\nu \rightarrow 2OH^\bullet \qquad\qquad r_H = -dc_H/dt = \phi I_a = \phi I_0 F \qquad\qquad (2\text{-}1)$$

H_2O_2 decay in pure water is given by the combination of the rate of energy absorption (usually the Beer-Lambert law) and the definition of the quantum yield (ϕ) as in reaction (2-1). The evaluation of the rate of energy absorption ($I_a = I_0F$) by the reactant, which undergoes photoreaction, depends on the reactor geometry and is performed by solving the radiation energy balance provided by the radiation source model. Thus the choice of the radiant source model is an important parameter in the kinetic study of a photochemical reaction. Many sophisticated radiation field models can be found in the existing literature (Alfano *et al.*, 1986a, 1986b). However, regarding the geometric characteristics of UV-BCR, I will focus on only two: the Radial model, and the Line Source with Spherical Emission (LSSE) model, developed by Jakob and Dranoff (1970).

2.2.1 Radial model

Here the light source is represented as an infinite line and all the light is presumed to be emitted from the line source only in radial direction; i.e., the problem is one-dimensional and the energy flux varies as 1/r. By solving the Beer-Lambert law for one dimension, the UV energy absorbed by H_2O_2 can be described by

$$I_a = I_0F_R = I_0(1-e^{-2.3D}) \tag{2-2}$$

where optical density is defined as the product of the light path length and attenuation coefficient as $D = \mu_H l = \varepsilon_H c_H l$. The path length of the light at a given wavelength l depends upon the type, geometry, and the construction material of the reactor as well as the transmitting medium and the type of the absorbing molecule, and thus needs to be determined for a given reacting system. If Eq. (2-2) is further rearranged and represented by

$$I_a = I_0F_R = 2.3\mu_H l_{eff}\eta I_0 \tag{2-3}$$

with

$$\eta = (1\text{-}e^{-2.3D})/(2.3\mu_H l) \tag{2-4}$$

where **h** is a fraction that becomes close to 1 for relatively small hydrogen peroxide concentrations, l_{eff} represents the empirical quantity called the effective path length that includes the above mentioned parameters.

2.2.2 LSSE model

In this model sometimes called the Multiple Point Source Summation Model (Bolton, 2000) developed by Jacob and Dranoff, the light source is still considered linear, but here of finite dimensions, with each of its points emitting radiation isotropically in all directions (Fig. 2.1). According to this model, the radiation flow rate absorbed is

$$I_a = \frac{2.3\mu_H \cdot 2\pi}{V} \int_0^H \int_{r_q}^{r_{RCT}} I(r,z) r\, dr\, dz \tag{2-5}$$

where I(r, z), the average point irradiation intensity is given by

$$I(r,z) = \frac{I_0'}{4\pi L} \int_{L_0}^{L_0+L} \frac{\exp\left(-2.3\mu_H (r-r_q) \cdot b\right)}{r^2 + (z-l)^2}\, dl \tag{2-6}$$

and the parameter *b* by

$$b = [r^2 + (z\text{-}z_l)^2]^{1/2} / r. \tag{2-7}$$

By combining Eqs.(2-5) and (2-6) the radiation flow rate absorbed can be represented by the final equation

$$I_a = I_0 \frac{2.3\mu_H N}{2L} = I_0 F_L \tag{2-8}$$

N being a global term that includes all the geometric parameters and absorbance, and is defined in the form

$$N = \int_0^H \int_{r_q}^{r_{RCT}} \int_{L_0}^{L_0+L} \frac{\exp\left(-2.3\mu_H(r-r_q)\cdot b\right)}{r^2+(z-l)^2} r\, dl\, dr\, dz \tag{2-9}$$

2.3 EXPERIMENTAL

2.3.1 Apparatus

All of the experiments were performed in the reactor system shown in Fig. 1.6. The geometry of reaction vessel is schematically depicted in Fig. 2.1. In all runs, the reactor was filled with 4 L of distilled water and after warming the lamp, the calculated amount of H_2O_2 concentrated solution was added into the vessel to obtain the desired initial concentrations (H_2O_2: 0.7-97.6 mmol/L). In experiments where the influence of gas bubbles on the degradation rate of hydrogen peroxide decomposition was checked, the air was introduced into the reactor through the air-stone coil gas distributor placed around the quartz tube at the bottom. The liquid phase was recirculated through the reactor by means of a magnetic pump (max capacity 18 L/min). The experiments were performed in a batch mode and the temperature was maintained at 25 °C (±1°C). Representative samples were taken at regular time intervals for H_2O_2 analysis.
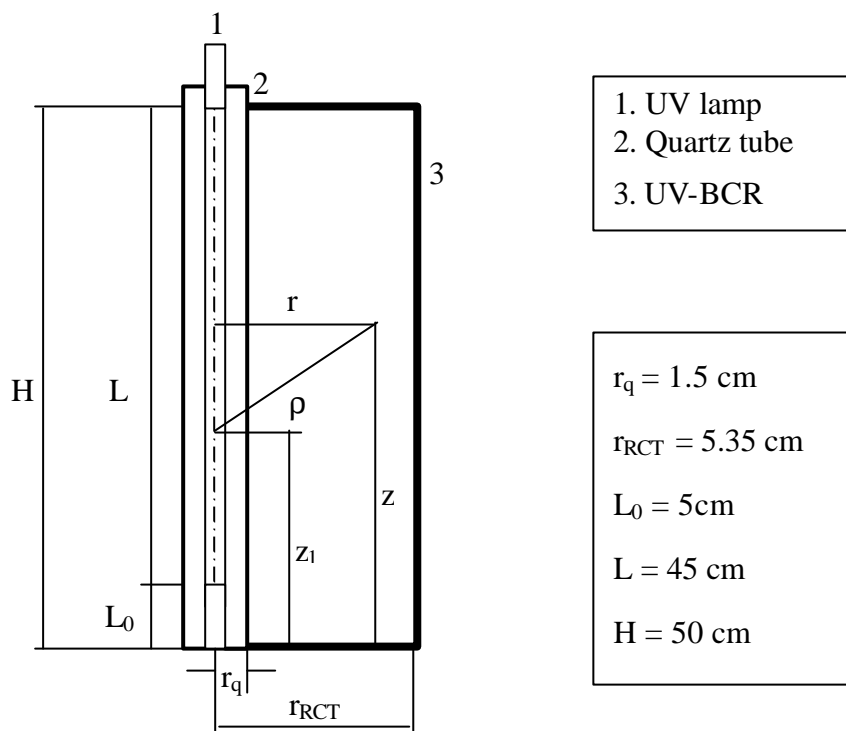
Figure 2.1. Geometric nomenclature of an annular UV-BC reactor.

2.3.2   Chemicals

All chemicals used in this work were purchased from Kanto Chemicals Co, and were used as received. PCE saturated solution used for spiking was prepared by continuously mixing the neat PCE with Milli-Q quality water for several weeks.

2.3.3 Analytical procedures

Liquid samples of H_2O_2 taken from the sampling port at regular time intervals were analyzed with permanganate titration using 785 DMP Titrino with 730 Sample Changer from Methrom.

2.4 RESULTS AND DISCUSSION

2.4.1 Hydrogen peroxide actinometry and Effective optical path length determination for Radial model

To obtain the effective path length for the UV-BCR, the degradation of hydrogen peroxide over a wide range of concentrations was performed. Data analysis shows that all the experimental results of hydrogen peroxide photolytic reactions can be fit to either a zero or a first order rate expression with high correlation coefficients.

When optical density is high enough (D > 2, the definition of total absorption conditions) more than 99% of the light emitted from the lamp is absorbed and H_2O_2 then acts as an actinometer (Fig. 2.2). Incident photon flux can then be calculated from the slope of the simplified relation $-dc_H/dt = \phi I_0$ for high light absorbance with $\phi = 1$ for the overall reaction of H_2O_2 photolysis. As shown in Fig. 2.2 the plot of c_H versus time yields a straight line, the value of which is equals the total absorbed photon flux.

Table 2.1. Equations used for photolysis kinetics. No bubbling, no reflection.

Hypothesis	Kinetic expression	Integrated form	Rct. order
General	$-dc_H/dt = \phi I_0(1-e^{-2.3D})$	$\ln(10^D-1) = \ln(10^{Do}-1) - 2.3\varepsilon l\phi I_0 t$	/
D>2	$-dc_H/dt = \phi I_0$	$c_H = c_{H,0} - \phi I_0 t$	0th
D<0.02	$-dc_H/dt = \phi I_0(2.3\varepsilon lc_H)$	$\ln(c_H/c_{H,0}) = -2.3\varepsilon l\phi I_0 t$	1st
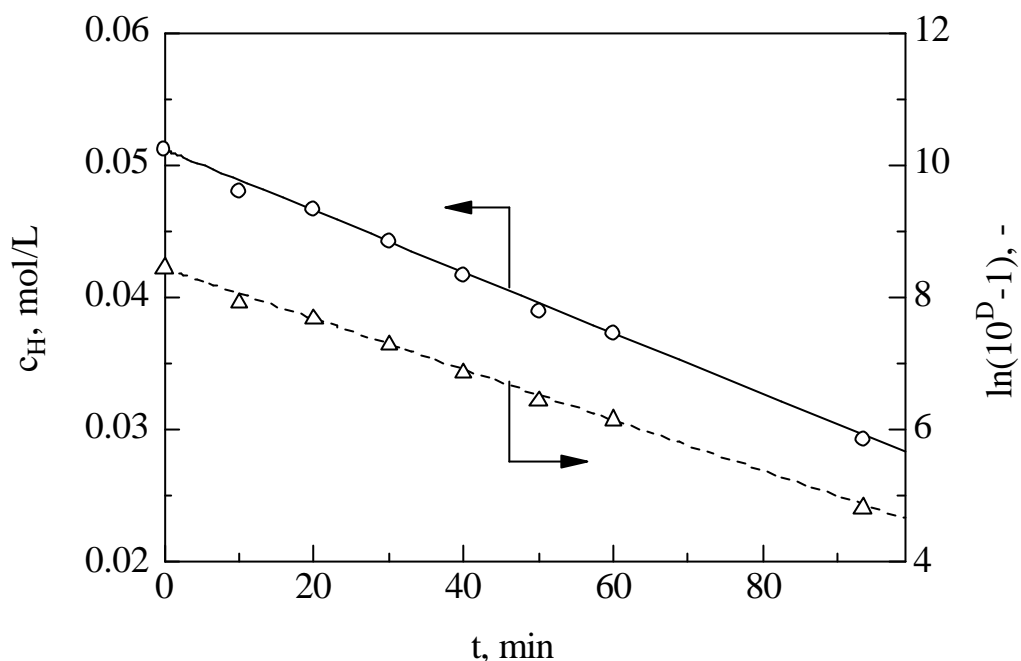
Figure 2.2. Actinometric run with 51.2 mmol/L of H_2O_2.

Table 2.2. Determination of incident photon rate and the effective path length using integrated form of Eq. (1). Radial model.

| c_{H2O2}, mmol L^{-1}	0.7	1.3	2.1	4.6	5.4	14	25.5	40	51.2
$2.3\varepsilon l\phi I_0$, $\times 10^{-4}$ s^{-1}	7.67	7.3	7.24	6.94	6.83	6.49	6.20	6.05	6.29
$I_0 l_{eff}$ / $I_0 l$, /		1.22	1.18	1.17	1.12	1.1	1.05	1.005	0.99	1.02

The plots of $\ln(10^D-1)$ *vs* time yielded a straight line (not shown) for all of the concentrations tested (Table 2.2.), the slope of which $(2.3\varepsilon l\phi I_0)$ yields the value "$l\phi I_0$". The incident photon rate (I_0) was determined as a mean value calculated from the slopes of 25.5, 40 and 51.2 mmol L^{-1} hydrogen peroxide concentrations. The zero order rate constants and the values obtained for ϕI_0 from plots of $\ln(10^D-1)$ *vs* time for those three concentrations were almost the same giving an average value of $\phi I_0 = 3.75$ μEi L^{-1} s^{-1}. As the overall quantum yield for

hydrogen peroxide decomposition (Baxendale and Wilson, 1957, Hunt and Taube, 1952) has been reported to be constant over the range of conditions applied here ($\approx$ 1), the increase in the calculated mean average photon rates with the decrease in hydrogen peroxide concentration could be attributed to the reflection of the UV light from the wall of the reactor (Table 2.2). The apparent increase in the photon rate will cause an increase in the light absorption rates as given by Eq.(2-2). Since the radiation emitted from the UV lamp (I_0) into a reactor of a given volume must be constant for constant lamp temperature, we can take its value as a reference, and the contribution of reflected light can then be determined as a quotient between the apparent mean photon rate with reflection and the incident photon rate (the photon rate determined at the conditions of total absorption) for all the concentrations tested (Table 2.2). By plotting the values of I_{app} versus transmittance, an empirical relation to account for reflection from the wall of the reactor was obtained by regression analysis (Fig. 2.3), and can be represented as a function of transmittance as

$$l_{eff} = l(1 + 0.24 \times 10^{-D}) \tag{2-10}$$

With increasing concentration more and more light gets absorbed before reaching the wall and the contribution of reflection decreases proportionally. When all of the light is absorbed before reaching the wall ($D \geq 2$), the effective path length is equal to the annulus of the UV-BCR (l). Since reactor volume increases with the square of the radius, the outer regions of the annulus can contribute heavily to the overall conversion in the vessel. This phenomena is important from an optimization point of view and will have to be considered in the kinetic modeling, especially when working under the conditions of high transmittance. This method for determination of the effective path length differs from the previously published methods (Nicole *et al*., 1990, Glaze *et al*., 1995, Zepp, 1978) in that it allows one to evaluate the evolution of the effective path length not only for low optical densities, but for the whole range of concentrations of absorbing species.
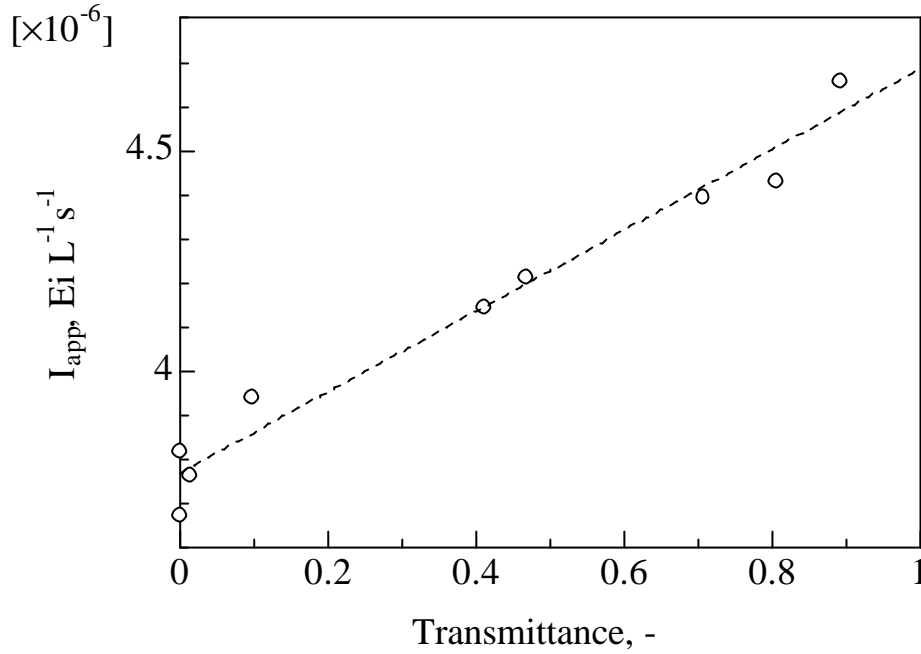
Figure 2.3. Apparent photon rate as a function of transmittance.

2.4.2 LSSE model

As stated above, when optical density is high enough ($D > 2$, the definition of total absorption conditions) the rate of energy absorption can be considered constant and independent of time, if H_2O_2 conversions are low and as far as conditions of total absorption apply. By combining Eqs. (2-1) and (2-8), after appropriate integration we can obtain

$$c_{H,0} - c_H = k_0 \cdot t = \phi I_0 \frac{2.3 \mu_H N}{2L} \cdot t = \phi I_0 F_L \cdot t \qquad (2\text{-}11)$$

From the slope of the plot of c_H versus time and parameters ϕ, μ_H, L and N previously known, the value of I_0 for LSSE model can be obtained. Applying the zero order rate constants for

H_2O_2 degradations as shown in Table 2.3, the incident photon rate for LSSE model was calculated to be 3.88 μEi L^{-1} s^{-1}. The value of F_L was calculated for the beginning and the end conditions of the reaction and did not change more than 1% in those measurements. Therefore the determination of I_0 in this way is justified. Parameter N was calculated for all the concentrations by numerical method, applying the "triplequad" routine from the Matlab program.

Table 2.3. Determination of the incident photon rate. LSSE model.

c_{H2O2}, mmol L^{-1}	25.5	40	51.2
k_0, mol L^{-1} s^{-1}	3.77×10^{-6}	3.7×10^{-6}	3.9×10^{-6}
N, cm^2	79.89	51.4	40.21
I_0, μEi L^{-1} s^{-1}	3.87	3.79	3.98
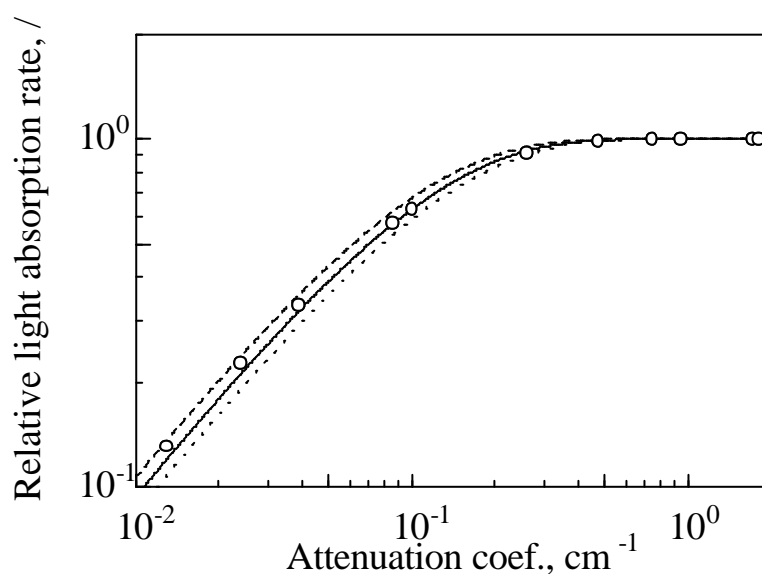
Figure 2.4. Relative light absorption rate as a function of attenuation coefficient (dotted line: Radial model; solid line: Radial model with effective path length; dashed line: LSSE model). Conditions: T = 25°C; I_0 = 3.75 μEi L^{-1} s^{-1}; pH_0 = 7.

The lines in Fig. 2.4 were constructed from the data in Table 2.2. For the radial model and

radial model with effective path length calculations, Eq. (2-2) with a UV reactor annulus and an annulus modified by the reflection coefficient (Eq. (2-10)) were used as a distance for light absorption, respectively. The nomenclature as shown in Fig. 2.1 was used for the determination of absorption rates via the LSSE model. The radial model predicts the lowest absorption rates, probably due to the neglect of reflection effects. These make apparent intensity in the reactor higher and thus make more photons available for the reaction. From the data presented in Tables 2.2 and 2.3, it can be concluded that both models can be used to calculate the light distribution and that there is no practical reason to apply the more complicated LSSE model. (See also Appendix A)

2.4.3 Light absorption in a heterogeneous reaction system

To account for the scattering of the light by the bubbles, the effective absorption coefficient (μ_e) can be employed. Yokota *et al.* (1981) studied the distributions of the light path inside the bubble column photochemical reactor by a Monte Carlo method and showed that for predictions of the light absorption rates the equations corresponding to the homogeneous system, but employing an effective absorption coefficient, can be used. They proposed the application of effective attenuation coefficient as

$$\mu_e = \mu(1 + (3.6/d_b)^{0.66}\, \varepsilon_G) \tag{2-12}$$

For modeling purposes the gas holdup and $K_L a$ for this specific reactor were calculated from Alibegic *et al.,* 2001, the bubble diameter from Bouaifi *et al.* (2001), and power consumption and interfacial area from well established relations as presented in Table 2.4.

### Table 2.4. Mass transfer characteristics of the UV-BCR

$\varepsilon_G = 4.595 u_G$	$K_L a = 1.003 u_G$	$d_b = 2.15 \times 10^{-3}(P_G/V_L)^{0.16}$	$a = 6\varepsilon_G/d_b$	$P_G/V_L = \rho_L g u_G$

To evaluate the increase of light absorption due to the presence of the bubbles, and to check

the applicability of the existing correlations for our system, we have performed a set of experiments, in which the degradation rates of hydrogen peroxide in the presence of the gas phase were measured. For this reason, the air was bubbled into the UV-BCR at a metered rate, and the apparent intensities were determined in a similar way as for the homogeneous phase. The expression for the effective attenuation coefficient as shown in Eq. (2-12) was inputted into Eq. (2-1), and after the appropriate integration, apparent mean intensities were obtained from the slope of the plot of $\ln(10^D-1)$ vs time in a similar procedure as for the homogeneous system. It was observed that the degradation rates of hydrogen peroxide were enhanced in the presence of the gas phase, confirming the effect of the light scattering. However, when the initial concentration of H_2O_2 was more than 25 mmol/L, the scattering effect was reduced. It was also observed that with the presence of a gas phase in the reactor, the effect of light reflection from the outer wall of the reactor was reduced, and the annulus of the UV-BCR was therefore used as a distance for the light absorption.
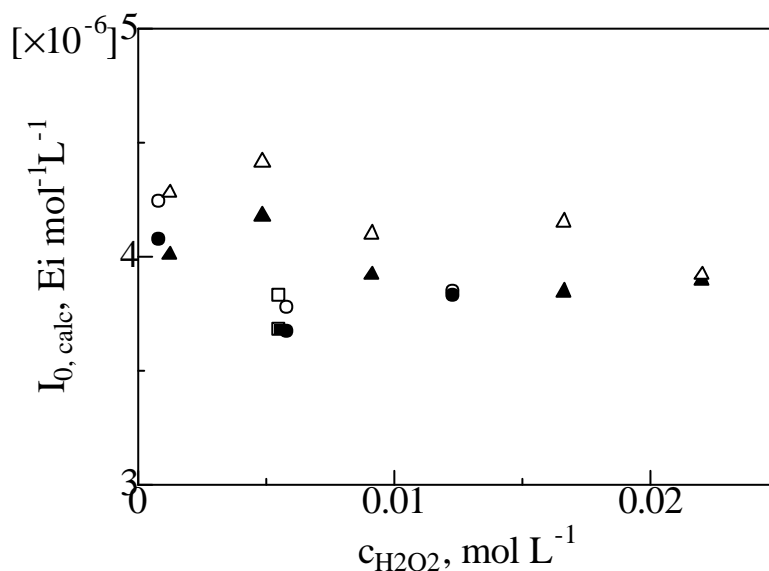
Figure 2.5. Calculated values of I_0 versus hydrogen peroxide concentration without (empty symbols) and with the application of effective attenuation coefficient (full symbols) for three different gas flow rates (triangles: Q = 1 L/min; squares: Q = 1.5 L/min; circles: Q = 2 L/min; T = 25°C; I_0 = 3.75 μEi L^{-1} s^{-1}; pH$_0$ = 7).

Figure 2.5 shows the incident photon rate calculated both with and without the application of the effective attenuation coefficient. It can be observed that by application of the effective coefficient, the values of the predicted incident photon flux for all gas flow rates are all close to the $4\,\mu Ei\,L^{-1}\,s^{-1}$, which does not differ much from the actinometric value ($3.75\,\mu Ei\,L^{-1}\,s^{-1}$). For the low gas flow rates used, the differences between the predicted values of I_0 are always less than 20 % even when calculated as for the homogeneous medium. It can be thus concluded that the application of effective attenuation coefficient is justified, and was consequently used in evaluation of absorbed light in the heterogeneous system.

2.4.4 H_2O_2 photolysis

The mechanism most commonly accepted for the photolysis of H_2O_2 is the cleavage of the molecule into hydroxyl radicals with a quantum yield of two OH radicals formed per quantum of radiation absorbed (Table 1.3). The rate of photolysis of aqueous H_2O_2

$$H_2O_2 \xrightarrow{\ h\nu\ } 2OH^{\bullet} \qquad\qquad r_{H2O2} = \phi_p I_a \qquad\qquad (2\text{-}1)$$
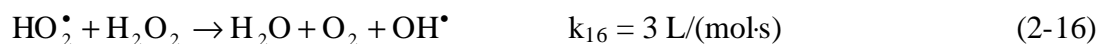
has been found to be pH dependent and increases with alkalinity. This might be due to the higher molar absorption coefficient (ε) of the peroxide anion at 254 nm (Table 1.4). Reaction (2-1) represents the first step in the reaction sequence, light absorption/initiation.

Other reactions in the process can be written as
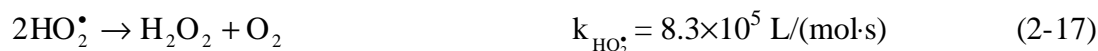
$$H_2O_2 \leftrightarrow HO_2^- + H^+ \qquad\qquad pKa=11.6 \qquad\qquad (2\text{-}13)$$

Propagation:

$$OH^{\bullet} + H_2O_2 \rightarrow HO_2^{\bullet} + H_2O \qquad\qquad k_{H2O2}=2.7\times10^7\ L/(mol{\cdot}s) \qquad\qquad (2\text{-}14)$$

$$OH^\bullet + HO_2^- \rightarrow HO_2^\bullet + OH^- \qquad\qquad k_{HO2^-}=7.5\times10^9 \text{ L/(mol·s)} \qquad (2\text{-}15)$$

$$HO_2^\bullet + H_2O_2 \rightarrow H_2O + O_2 + OH^\bullet \qquad\qquad k_{16} = 3 \text{ L/(mol·s)} \qquad (2\text{-}16)$$

Termination:

$$2HO_2^\bullet \rightarrow H_2O_2 + O_2 \qquad\qquad k_{HO_2^\bullet} = 8.3\times10^5 \text{ L/(mol·s)} \qquad (2\text{-}17)$$

$$2OH^\bullet \rightarrow H_2O_2 \qquad\qquad k_{HO^\bullet} =5.5\times10^9 \text{ L/(mol·s)} \qquad (2\text{-}18)$$

$$OH^\bullet + HO_2^\bullet \rightarrow H_2O + O_2 \qquad\qquad k_{19} = 6.6\times10^9 \text{ L/(mol·s)} \qquad (2\text{-}19)$$

and illustrate the importance of optimization of hydrogen peroxide concentration. In general, the net reaction from this kinetic scheme results in the overall quantum yield for hydrogen peroxide destruction of 1, twice the primary quantum yield ($\phi_p = 0.5$).

Generated at high (local) concentration (caused by high light flux conditions) hydroxyl radicals will readily dimerize to H_2O_2 (Eq. 2-18) resulting in the quantum yield less than 1. If an excess of H_2O_2 is used, OH radical will produce hydroperoxyl radicals (Eq. 2-14) which are much less reactive and do not appear to contribute to the oxidative degradation of organic substances.
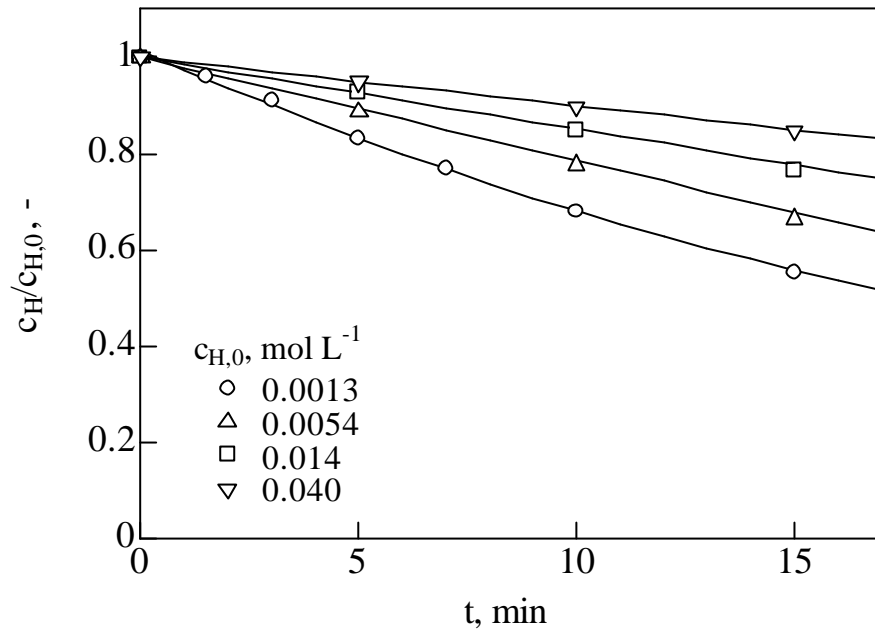
Figure 2.6. Decomposition of hydrogen peroxide in the UV/H_2O_2 process. Influence of the initial hydrogen peroxide concentration. Conditions: $T = 25°C$; $I_0 = 3.75$ μEi L^{-1} s^{-1}; $pH_0 = 7$.

Figure 2.6 shows the influence of the initial hydrogen peroxide concentration on the H_2O_2 degradation rate. It can be observed in Fig. 2.6 and in Table 2.2 that an increase in the initial hydrogen peroxide concentration decreases its degradation rate. This indicates that in addition to decreasing the pollutant degradation rate, increasing the initial hydrogen peroxide concentration will lead to a high level of hydrogen peroxide residual in the treated water and therefore to an increase in the operating cost. This can be explained in two ways. With the increasing H_2O_2 concentration, the absorption of UV light increases leading to a subsequent production of OH radicals. However, the reflection of the UV light from the wall becomes lower with increasing concentration and so its contribution to the relative increase in light intensity in reactor starts to decline. Also, as the H_2O_2 concentration increases, the UV light becomes absorbed in a narrower area around the UV light. Since reactor volume increases with the square of the radius, the outer regions of the annulus contribute heavily to the overall conversion in the vessel. For the reasons stated, it is important that the radiation field in the

44

reactor is uniform and that light is absorbed homogeneously over the annulus of the reactor.

2.5 CONCLUSIONS

In this chapter the light absorption characteristics of the UV-BCR were evaluated. It was shown that with a properly estimated effective path length for the UV light absorption, the simpler, one dimensional, Radial model can be successfully applied for the light distribution and absorption predictions. In addition, the kinetics of hydrogen peroxide decomposition showed that due to the radical nature of the decomposition kinetics, the UV light power and initial concentrations should be optimized for a given reactor geometry, in order to optimize OH radical formation. If light is applied strongly enough to produce high local concentrations of OH radical, these will readily dimerize back to hydrogen peroxide, reducing the overall efficiency of the process.